

## RESEARCH PAPER

# Identification of *N*-arachidonoyl dopamine as a highly biased ligand at cannabinoid CB<sub>1</sub> receptors

### Correspondence

Mark Connor, 2 Technology Place,  
Macquarie University, NSW 2109,  
Australia.

E-mail: mark.connor@mq.edu.au

### Received

9 November 2014

### Revised

13 September 2015

### Accepted

17 September 2015

William J. Redmond<sup>1</sup>, Erin E. Cawston<sup>2</sup>, Natasha L. Grimsey<sup>2</sup>,  
Jordyn Stuart<sup>1</sup>, Amelia R. Edington<sup>1</sup>, Michelle Glass<sup>2</sup> and Mark Connor<sup>1</sup>

<sup>1</sup>Department of Biomedical Sciences, Faculty of Medicine and Health Sciences, Macquarie University, NSW 2109, Australia, and <sup>2</sup>Department of Pharmacology and Clinical Pharmacology, and Centre for Brain Research, University of Auckland, Auckland, New Zealand

## BACKGROUND AND PURPOSE

*N*-arachidonoyl dopamine (NADA) has been identified as a putative endocannabinoid, but there is little information about which signalling pathways it activates. The purpose of this study was to identify the signalling pathways activated by NADA *in vitro*.

## EXPERIMENTAL APPROACH

Human or rat cannabinoid CB<sub>1</sub> receptors were expressed in AtT20, CHO or HEK 293 cells. NADA displacement of radiolabelled cannabinoids, and CB<sub>1</sub> receptor mediated activation of K channels or ERK phosphorylation, release of intracellular calcium ([Ca]<sub>i</sub>) and modulation of adenylyl cyclase were measured in addition to NADA effects on CB<sub>1</sub> receptor trafficking.

## KEY RESULTS

At concentrations up to 30 μM, NADA failed to activate any signalling pathways via CB<sub>1</sub> receptors, with the exception of mobilization of [Ca]<sub>i</sub>. The elevations of [Ca]<sub>i</sub> were insensitive to pertussis toxin, and reduced or abolished by blockers of G<sub>q/11</sub>-dependent processes including U73122, thapsigargin and a peptide antagonist of G<sub>q/11</sub> activation. Prolonged NADA incubation produced modest loss of cell surface CB<sub>1</sub> receptors. The prototypical cannabinoid agonist CP55940 signalled as expected in all assays.

## CONCLUSIONS AND IMPLICATIONS

NADA is an ineffective agonist at most canonical cannabinoid receptor signalling pathways, but did promote mobilization of [Ca]<sub>i</sub> via G<sub>q</sub>-dependent processes and some CB<sub>1</sub> receptor trafficking. This signalling profile is distinct from that of any known cannabinoid, and suggests that NADA may have a unique spectrum of effects *in vivo*. Our results also indicate that it may be possible to identify highly biased CB<sub>1</sub> receptor ligands displaying a subset of the pharmacological or therapeutic effects usually attributed to CB<sub>1</sub> ligands.

## Abbreviations

2-AG, 2-arachidonoyl glycerol; AtT20-rCB<sub>1</sub>, mouse pituitary tumour cells stably transfected with HA-tagged rat CB<sub>1</sub> receptors; [Ca]<sub>i</sub>, intracellular calcium; CHO-hCB<sub>1</sub>, CHO cells stably transfected with HA-tagged human CB<sub>1</sub> receptors; FSK, forskolin; GIRK (K<sub>ir</sub>3), G protein gated inwardly rectifying K channel; HA-hCB<sub>1</sub>, haemagglutinin-tagged human CB<sub>1</sub> receptor; HA-rCB<sub>1</sub>, haemagglutinin-tagged rat CB<sub>1</sub> receptor; PBS-T, PBS supplemented with 0.2% Tween

## Tables of Links

TARGETS	
<b>GPCRs<sup>a</sup></b>	<b>Enzymes<sup>c</sup></b>
β <sub>2</sub> -adrenoceptor	Adenylyl cyclase (AC)
CB <sub>1</sub> receptor	ERK1
CB <sub>2</sub> receptor	ERK2
<b>Ion channels<sup>b</sup></b>	
GIRK (K <sub>ir</sub> 3)	
TRPV1	

LIGANDS	
2-AG	Forskolin (FSK)
Arachidonic acid	NADA
ATP	SR141716A
Bradykinin	Thapsigargin
Capsaicin	U73122
CP55940	

These Tables list key protein targets and ligands in this article which are hyperlinked to corresponding entries in <http://www.guidetopharmacology.org>, the common portal for data from the IUPHAR/BPS Guide to PHARMACOLOGY (Pawson *et al.*, 2014) and are permanently archived in the Concise Guide to PHARMACOLOGY 2013/14 (<sup>a,b,c</sup>Alexander *et al.*, 2013a,b,c).

## Introduction

Cannabinoid CB<sub>1</sub> and CB<sub>2</sub> receptors have important roles in modulating neuronal and immune system function. CB<sub>1</sub> receptors are expressed throughout the brain in presynaptic compartments and generally act there to modify the release of other neurotransmitters (Mackie, 2005; Lovinger, 2008). Endogenous cannabinoid tone controlling moment-to-moment communication has been recognized at many synapses, but persistent elevation of endocannabinoid levels is also observed following significant pathophysiological stimuli (Hohmann *et al.*, 2005). The principle endocannabinoids are 2-arachidonoyl glycerol (2-AG) and anandamide, although candidate molecules such as virodhamine, noladin ether and NADA have also been identified (Alexander and Kendall, 2007).

CB<sub>1</sub> receptors are unusually pleiotropic in their signalling. Although principally exerting their actions through G<sub>i</sub>/G<sub>o</sub>-type G proteins, CB<sub>1</sub> receptors can also couple to G<sub>s</sub> to stimulate AC activity (Glass and Felder, 1997), and to G<sub>q</sub> to mobilize intracellular calcium ([Ca]<sub>i</sub>) via phospholipase C (PLC) (Lauckner *et al.*, 2005). The physiological consequences of this abundance of potential signalling avenues for CB<sub>1</sub> receptors remains an area of intense investigation, particularly in light of the idea that different ligands may preferentially activate one set of effectors over another (Hudson *et al.*, 2010; Laprairie *et al.*, 2014; Khajehali *et al.*, 2015).

NADA was identified as a CB<sub>1</sub> agonist *in vitro* (Bisogno *et al.*, 2000) and subsequently identified *in vivo* (Huang *et al.*, 2002; Bradshaw *et al.*, 2006), although much subsequent work has focussed on its activity as an agonist of TRPV1, ion channels found in both brain and peripheral sensory neurons. In brain, NADA is most abundant in regions containing the cell bodies or terminals of dopaminergic neurons (Huang *et al.*, 2002; Bradshaw *et al.*, 2006; Hu *et al.*, 2009), and NADA has been reported to modulate GABAergic neurotransmission via both CB<sub>1</sub>- and TRPV1-dependent mechanisms (Marinelli *et al.*, 2007; Fawley *et al.*, 2014; Freestone *et al.*, 2014).

The initial report of NADA activity at CB<sub>1</sub> receptors measured changes in [Ca]<sub>i</sub> in N18TG2 neuroblastoma cells, with NADA producing an elevation of [Ca]<sub>i</sub> similar to that of the synthetic cannabinoid HU-210. The elevations of [Ca]<sub>i</sub> were blocked by the CB<sub>1</sub> antagonist SR141716A. However, the mechanism of NADA-induced elevations of [Ca]<sub>i</sub> in N18 cells was not

determined. Surprisingly, the report of Bisogno *et al.* (2000) remains the only cellular study of the signalling mechanisms potentially underlying NADA actions. In this study, we have examined NADA signalling through recombinant CB<sub>1</sub> receptors expressed in several cell lines. Intriguingly, we found that NADA did not modulate K channels, AC or ERK phosphorylation in cell lines expressing CB<sub>1</sub> receptors; in fact, the only signalling pathway activated by NADA was an elevation of [Ca]<sub>i</sub> mediated by pertussis toxin-insensitive G proteins. Thus, the endocannabinoid NADA appears to have a highly pathway-biased CB<sub>1</sub> receptor signalling profile, unique amongst the cannabinoid agonists described to date.

## Methods

### Cell culture

Experiments utilized human or rat CB<sub>1</sub> tagged at the N-terminus with three haemagglutinin sequences [haemagglutinin-tagged human CB<sub>1</sub> receptor (HA-hCB<sub>1</sub>) and haemagglutinin-tagged rat CB<sub>1</sub> receptor (HA-rCB<sub>1</sub>)] stably transfected into HEK 293, CHO or AtT20 cells. HEK 293-hCB<sub>1</sub> (Cawston *et al.*, 2013) cells were used for AC, phosphoERK, internalization and binding assays. CHO cells stably transfected with HA-tagged human CB<sub>1</sub> receptors (CHO-hCB<sub>1</sub>) (Grimsey *et al.*, 2010) were used for measurements of changes in [Ca]<sub>i</sub>, cAMP and receptor internalization. AtT20-rCB<sub>1</sub> cells (Mackie *et al.*, 1995) were used for assays of G protein-gated inwardly rectifying K channel (GIRK)-mediated hyperpolarization. HEK 293 FLPIn-TREx cells transfected with hTRPV1 were used to assess the efficacy of NADA at a known effector. N18TG2 cells (obtained from the European Collection of Cell Cultures) were used for assays of [Ca]<sub>i</sub>. N18TG2, HEK 293 and AtT20 cells were cultivated in DMEM supplemented with 10% FBS, 100 U penicillin and 100 µg streptomycin ·mL<sup>-1</sup>. HEK 293-hCB<sub>1</sub> cell media contained zeocin, 250 µg·mL<sup>-1</sup>, media for AtT20 cells was supplemented with 400 µg·mL<sup>-1</sup> G418. HEK 293-hTRPV1 cells were grown in media supplemented with hygromycin (150 µg·mL<sup>-1</sup>) and blasticidin (10 µg·mL<sup>-1</sup>). CHO-hCB<sub>1</sub> cells were cultivated in DMEM/F12-HAM media supplemented as for HEK 293-HA-hCB<sub>1</sub>. Cells were maintained in 5% CO<sub>2</sub> at

37°C in a humidified atmosphere. Cells were grown in 75 mm<sup>2</sup> flasks and passaged when 80–90% confluent.

### Binding assays

HEK 293-hCB<sub>1</sub> cells were grown to 90–100% confluence in 175 cm<sup>2</sup> flasks and harvested in ice-cold PBS with 5 mM EDTA. Cells were centrifuged at 200 × *g* for 10 min and the pellet frozen at –80°C until required. Pellets were thawed with Tris-sucrose buffer (50 mM Tris-HCl, pH 7.4, 200 mM sucrose, 5 mM MgCl<sub>2</sub>, 2.5 mM EDTA) and homogenized with a glass homogenizer. The homogenate was centrifuged at 1000 × *g* for 10 min at 4°C and the pellet discarded. The supernatant was then centrifuged at 27 000 × *g* for 30 min at 4°C. The final pellet was resuspended in a minimal volume of Tris-sucrose buffer, aliquoted and stored at –80°C. Protein concentration was determined using the DC protein assay kit (Bio-Rad, Hercules, CA, USA) following the manufacturer's protocol. Membranes (20 µg per point) were resuspended in binding buffer (50 mM HEPES, 1 mM MgCl<sub>2</sub>, 1 mM CaCl<sub>2</sub>, 0.2% (w v<sup>-1</sup>) BSA; ICP Bio, New Zealand, pH 7.4) and incubated with either [<sup>3</sup>H]-CP55940 (2.5 nM) or [<sup>3</sup>H]-SR141716A (1 nM, both PerkinElmer, Waltham, MA, USA) and a range of NADA concentrations at 30°C for 60 min. Non-specific binding was determined in the presence of 1 µM SR141716A. GF/C Harvest Plates (PerkinElmer) were pre-soaked in 0.1% polyethylenimine and then washed with 100 µL ice-cold wash buffer (50 mM HEPES pH 7.4 500 mM NaCl, 0.1% BSA) before filtration of samples, which were then subjected to three additional 200 µL washes in ice-cold wash buffer. Harvested plates were dried overnight at 24°C, 50 µL of scintillation fluid was added to each well and plates were read 30 min later for 2 min per well in a Microbeta Trilux (PerkinElmer).

### Intracellular calcium measurements

[Ca]<sub>i</sub> was measured with the Calcium 5 kit from Molecular Devices (Sunnyvale, CA, USA) using a FlexStation 3 Microplate Reader (Molecular Devices), as outlined in Redmond *et al.* (2014). Briefly, N18TG2, CHO-hCB<sub>1</sub> or HEK 293-hTRPV1 cells from an 80–90% confluent 75 mm<sup>2</sup> flask were resuspended in L-15 medium supplemented with 1% FBS, 100 U penicillin and 100 µg streptomycin mL<sup>-1</sup> and plated in 96-well black-walled plates (Corning, Castle Hill, Australia). Cells were incubated overnight in humidified room air at 37°C. hTRPV1 expression was induced with 1 µg·mL<sup>-1</sup> tetracycline at least 4 h before the assay. Calcium 5 dye dissolved in a HBS containing (in mM): NaCl 140, KCl 5.33, CaCl<sub>2</sub> 1.3, MgCl<sub>2</sub> 0.5, HEPES 22, Na<sub>2</sub>HPO<sub>4</sub> 0.338, NaHCO<sub>3</sub> 4.17, KH<sub>2</sub>PO<sub>4</sub> 0.44, MgSO<sub>4</sub> 0.4, glucose 10, probenidicid 2.5 (pH to 7.3, osmolarity 330 ± 5 mosmol) was loaded into each well and incubated at 37°C for at least 1 h before the assay. Fluorescence was measured every 2 s ( $\lambda_{\text{excitation}} = 485 \text{ nm}$ ,  $\lambda_{\text{emission}} = 525 \text{ nm}$ ). Drugs were dissolved in HBS and added after at least 2 min of baseline recording in volumes of 20–50 µL. Assays were carried out at 37°C unless otherwise noted. NADA produced small elevations of [Ca]<sub>i</sub> in untransfected CHO cells. These changes in [Ca]<sub>i</sub> were similar to those produced by equivalent concentrations of arachidonic acid in both wild-type and CHO-hCB<sub>1</sub> cells, and were not sensitive to inhibitors of PLC (Felder *et al.*, 1993; data not shown). When group responses are expressed as % change in RFU, data were corrected by subtracting the non-specific changes in [Ca]<sub>i</sub> seen in wild-type CHO cells. These effects were less than 30% of the equivalent

response following CB<sub>1</sub> receptor activation. On rare occasions, CHO-hCB<sub>1</sub> cells failed to respond to cannabinoids with an elevation of [Ca]<sub>i</sub>. The reasons for this are unknown, but may reflect unusually high densities of plated cells.

### K channel measurements in AtT20 cells

Changes in membrane potential were determined using the blue membrane potential dye (Molecular Devices) in a FlexStation 3, as outlined in Knapman *et al.* (2013). AtT20-rCB<sub>1</sub> cells from an 80–90% confluent 75 mm<sup>2</sup> flask were resuspended in L-15 medium supplemented with 1 % FBS, 100 U penicillin and 100 µg streptomycin mL<sup>-1</sup> and plated in 96-well black-walled plates in a volume of 100 µL per well. Cells were incubated overnight in humidified room air at 37°C. Membrane potential dye was dissolved in a modified HBS where KCl was omitted and loaded into each well and incubated at 37°C for at least 1 h before the assay. Fluorescence was measured every 2 s ( $\lambda_{\text{excitation}} = 530 \text{ nm}$ ,  $\lambda_{\text{emission}} = 565 \text{ nm}$ ). Assays were carried out at 37°C, and drugs were added in volumes of 25–50 µL after at least 2 min of baseline recording.

### cAMP measurement

Cellular cAMP levels were measured as previously described (Cawston *et al.*, 2013). Briefly, the pcDNA3L-His-CAMYEL plasmid (ATCC, Manassas, VA, USA) was transfected into HEK 293-hCB<sub>1</sub> cells using linear polyethyleneimine (m.w. 25 kDa) (Polysciences, Warrington, PA, USA). Twenty-four hours after transfection cells were re-plated in poly-L-lysine (0.2 mg·mL<sup>-1</sup> in PBS) (Sigma-Aldrich, St Louis, MO, USA) coated with CulturPlate™-96 (PerkinElmer) at a density of 55 000–80 000 cells per well. After 24 h, cells were serum-starved in HBSS containing 1 mg·mL<sup>-1</sup> BSA, pH 7.4 for 30 min before assay. Five minutes before the addition of drug or vehicle dissolved in HBSS plus 1 mg·mL<sup>-1</sup> BSA cells were treated with 5 µM coelenterazine-h (Promega, Madison, WI, USA). Emission signals were detected simultaneously at 460/25 nM (RLuc) and 560/25 nM (YFP), immediately following drug addition with a Victor-Lite plate reader (PerkinElmer) at 37°C. Raw data are presented as an inverse BRET ratio of emission at 460/535 so that an increase in ratio correlates with an increase in cAMP production.

Modulation of forskolin (FSK)-stimulated AC activity in CHO-hCB<sub>1</sub> cells was measured as described in detail in Knapman *et al.* (2014). In CHO cells, stimulation of AC hyperpolarizes cells, this can be reversed by agonists for G<sub>i/o</sub>-coupled receptors. Briefly, CHO-hCB<sub>1</sub> cells were prepared for membrane potential measurements using the blue membrane potential dye as outlined above. After 2 min of baseline recording, FSK was added to the cells in a volume of 20 µL, either with or without NADA or CP55940. Changes in membrane potential were measured 5 min after drug addition. In some experiments, cells were treated overnight with 200 ng·mL<sup>-1</sup> pertussis toxin.

### CB<sub>1</sub> receptor cell surface expression

Surface hCB<sub>1</sub> receptor expression was determined by utilizing a live cell antibody feeding technique and quantified via the ImageXpress Micro XLS automated fluorescent microscope (Molecular Devices) as previously described (Grimsey *et al.*, 2008). In brief, HEK 293-hCB<sub>1</sub> or CHO-hCB<sub>1</sub> cells were seeded at 30 000 or 22 000 cells per well (respectively) in poly-L-lysine treated 96-well, flat bottom clear plates (Nunc, Roskilde, Denmark).

Untransfected HEK 293 and CHO cells and HEK 293 cells transfected with HA-tagged human  $\beta_2$  adrenoreceptors were also used in control experiments and treated equivalently. Approximately 24 h later, cells were equilibrated in DMEM (HEK 293-hCB<sub>1</sub>) or DMEM/F12-HAM (CHO-hCB<sub>1</sub>) supplemented with 1 mg·mL<sup>-1</sup> BSA (assay media) for 30 min at 37°C. For experiments assessing CB<sub>1</sub> receptor internalization with 1 h stimulation, cells were subsequently incubated with anti-mouse monoclonal HA11 primary antibody (MMS-101P, Covance, Princeton, NJ, USA) diluted 1:500 in assay media at 37°C for 30 min. After one wash with assay media, NADA at various concentrations and/or CP55940 at its approximate EC<sub>80</sub> for internalization (1 nM for HEK 293-hCB<sub>1</sub>, 3.2 nM for CHO-hCB<sub>1</sub>; data not shown) were applied for 60 min at 37°C. Following drug incubation, plates were cooled rapidly on ice to prevent any further receptor trafficking, then incubated with Alexa Fluor® 488-conjugated goat anti-mouse secondary antibody (Life Technologies, Mulgrave, Victoria, Australia) diluted 1:300 in assay media at room temperature for 30 min. Cells were washed once in assay media, fixed with 4% paraformaldehyde and stained with Hoechst 33258 (Life Technologies) diluted 1:500 in PBS with 0.2% Triton-X (PBS-T). For 6 h concentration-response and timecourse experiments, cells were treated as above (specific time points and drug concentrations noted in the text and figures) with the exception that primary antibody incubation was not carried out before drug incubation. Instead, the primary antibody was applied at the conclusion of drug incubation and incubated for 30 min at room temperature after rapidly cooling of the plates on ice to prevent further receptor trafficking. After being washed with assay media and fixed with paraformaldehyde, secondary antibody was incubated for 3 h at room temperature (diluted 1:400 in immunobuffer, PBS-T with 1% normal goat serum and 0.4 mg·mL<sup>-1</sup> merthiolate; Merck, Darmstadt, Germany). Cells were then washed with PBS-T before Hoechst staining as described above.

Images of the cells were acquired with a ImageXpress Micro XLS microscope (10× objective, four images per well) and experimental effects quantified using MetaMorph (v.7.8.0.0, Molecular Devices) by calculating the intensity of fluorescent labelling above background per cell (Grimsey *et al.*, 2008).

### ERK1/2 measurements

AlphaScreen® SureFire® Phospho(p)ERK1/2(Thr202/Tyr204) assay kits (PerkinElmer) were utilized following the manufacturer's protocol; 40 000 HEK 293-hCB<sub>1</sub> cells per well were seeded into poly-L-lysine treated 96-well plates (Corning) and incubated at 37°C, 5% CO<sub>2</sub> and 95% humidity for 24 h. Cells were serum-starved in 50  $\mu$ L DMEM supplemented with 1 mg·mL<sup>-1</sup> BSA overnight before drug treatment. All drugs were added at 2× concentration in DMEM-BSA and incubated for the times indicated. Assay plates were put onto ice, media/drug removed and 30  $\mu$ L of lysis buffer added followed by agitation of the plates for 10 min at RT. Cell lysate (5  $\mu$ L) was transferred into a white 96-well low volume plate (PerkinElmer) and 7  $\mu$ L detection mix was added. Plates were sealed, wrapped with foil and incubated for 2–4 h at RT, and fluorescent signals detected on an EnSpire reader (PerkinElmer) using the manufacturer-defined AlphaScreen settings.

### Data analysis

Analysis for all experiments was performed with GraphPad Prism (Version 5.02, GraphPad Software, Inc., La Jolla, CA, USA) and

SigmaPlot (v.11.0, Systat Software, Chicago, IL, USA). Binding assay data were analysed by fitting a one-site competition curve, and  $K_i$  was calculated using the previously determined  $K_d$  of 2.5 nM [<sup>3</sup>H]-CP55940 or 1 nM [<sup>3</sup>H]-SR141716A. For ERK 1/2 phosphorylation data, statistical significance was determined at 5 min. Raw data for the cAMP assays were usually fitted with one-phase association curves for each replicate, and plateau values were obtained. In the case of NADA attenuation of FSK-stimulated cAMP by CP55940, data were analysed using 'area under the curve' analysis in GraphPad Prism. Paired *t*-tests were used when comparing two datapoints, one-way ANOVA repeated measures for more than two data points with one independent variable. The response to drugs in assays of [Ca]<sub>i</sub> and membrane potential was expressed as a percentage change over the baseline averaged for 30 s immediately before drug addition. Changes produced by parallel solvent blanks were subtracted before normalization. Concentration–effect data were fit to a four-parameter logistic Hill equation to derive the EC<sub>50</sub> values. A two-way ANOVA was used to analyse the effect of NADA on CP55940 concentration–effect curves generated in this assay. Unless otherwise noted, data represent the mean  $\pm$  SEM of at least five independent experiments, each conducted in duplicate or triplicate.

Statistical significance was defined as  $P < 0.05$ .

### Drugs and reagents

HEK 293 FlpInTRex-hTRPV1 cells were kind gift from Peter McIntyre and were generated as described for cells expressing rTRPV1 (Veldhuis *et al.*, 2012). Drugs were made up in ethanol or DMSO and diluted to give a final concentration of solvent of 0.05–0.1%. U73122 and G<sub>q</sub> Palpeptide were made fresh before each use and were diluted in DMSO and water respectively. NADA and other endocannabinoids were purchased from Biomol (Plymouth Meeting, PA, USA), Cayman Chemicals (Ann Arbor, MI, USA) or Ascent Scientific, (Bristol, UK). Palpeptides were custom synthesized by Genscript (Piscataway, NJ, USA). Other drugs were from Tocris Cookson (Bristol, UK) or Cayman Chemicals unless otherwise noted. Cell culture media, buffers, antibiotics and general chemicals were from Life Technologies, Sigma-Aldrich or InvivoGen (San Diego, CA, USA).

## Results

NADA has been reported to act as a CB<sub>1</sub> agonist in tissue and cell lines derived from both rats and mice (Bisogno *et al.*, 2000; Marinelli *et al.*, 2007; Fawley *et al.*, 2014). Therefore, we initially examined its ability to modify canonical CB<sub>1</sub> receptor G<sub>1/o</sub>-mediated signalling. The classical CB<sub>1</sub> agonist CP55940-induced concentration-dependent GIRK-mediated hyperpolarization ( $pEC_{50}$  8.2  $\pm$  0.3) in AtT20-rCB<sub>1</sub> cells. However, when NADA (30–100  $\mu$ M) was applied to AtT20-rCB<sub>1</sub>, it did not produce a change in membrane potential by itself, nor did it modify the GIRK-mediated hyperpolarization produced by the CB<sub>1</sub> agonist CP55940 ( $pEC_{50}$  8.0  $\pm$  0.3 in the presence of 30  $\mu$ M NADA, Figure 1, two-way ANOVA, significant effect of CP55940 concentration,  $P < 0.0001$ , no effect of NADA,  $P = 0.36$ ).

CB<sub>1</sub> receptors couple very efficiently to inhibition of AC activity, and in some circumstances to stimulation of the enzyme (Glass and Felder, 1997; Bonhaus *et al.*, 1998). Therefore, we examined

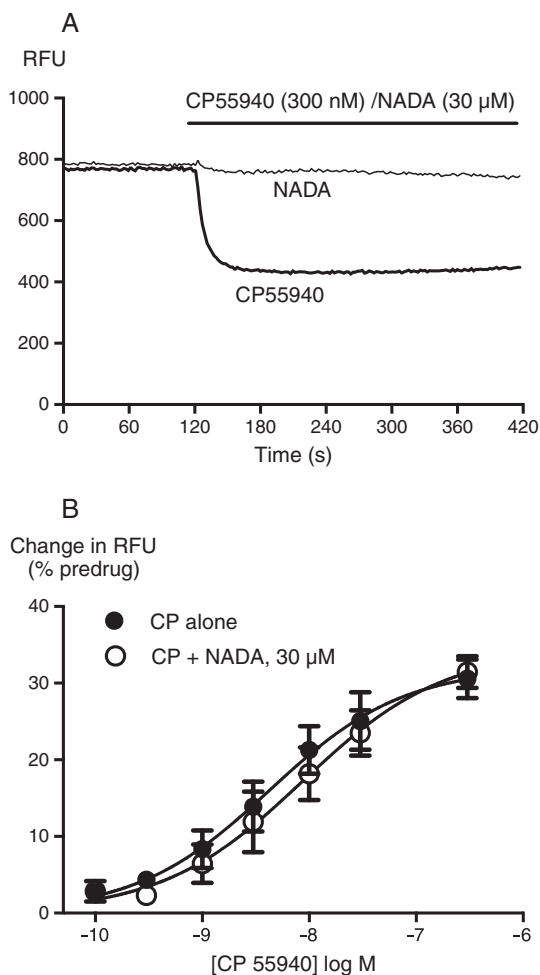


**Figure 1**

NADA does not activate K channels in AtT20 cells. GIRK activation was determined as described in the Methods. (A) Raw traces showing changes in fluorescent signal from the membrane potential dye (raw fluorescence units, RFU) in AtT20-rCB<sub>1</sub> cells during application of CP55940 but not NADA. Drug was added for the duration of the bar; the traces are representative of at least five independent experiments. (B) Concentration-response curves for CP55940 activation of GIRK in AtT20-rCB<sub>1</sub> cells in the presence and absence of 30 μM NADA. Data represent the mean ± SEM of at least five independent experiments performed in duplicate; pooled data were fit with a four-parameter logistic equation. There was no difference in the potency or maximal effect of CP55940 between control conditions or in the presence of NADA.

the ability of NADA to modify cAMP in HEK 293-hCB<sub>1</sub> cells. At concentrations up to 10 μM, NADA did not modify basal ( $P=0.777-0.940$ ,  $n=7$ ) or FSK-stimulated ( $P=0.390-0.976$ ,  $n=3$ ) cAMP production in HEK 293-hCB<sub>1</sub> cells. At 32 μM, NADA did not modify basal cAMP production (Figure 2A); however, when co-applied with 10 μM FSK, it modestly but significantly increased cAMP levels above that of FSK alone ( $P < 0.001$ ,  $n=10$ ) (Figure 2B). To ensure this was receptor-mediated, NADA was tested in HEK 293 wild-type cells; in these cells, NADA (32 μM) also produced a small increase in FSK-stimulated cAMP

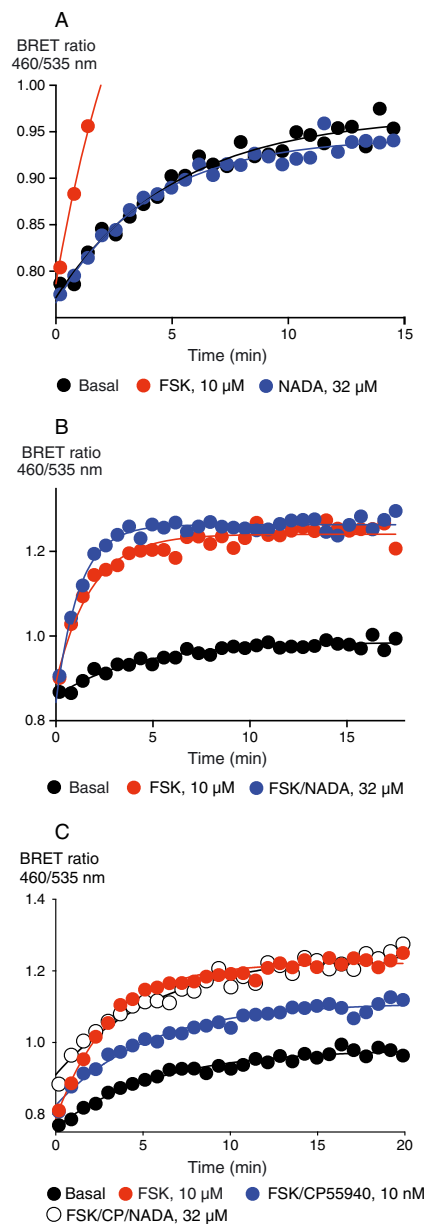


**Figure 2**

NADA does not modulate cAMP accumulation via CB<sub>1</sub> receptors in HEK 293-hCB<sub>1</sub> cells. Cellular cAMP levels were determined as outlined in the Methods. Figures are representative time plots of BRET emissions expressed as a ratio. Each point represents the mean of duplicate determinations. (A) NADA does not affect basal levels of cAMP, while FSK produces a robust increase (note truncated axis). Data are representative of four independent experiments. (B) NADA (32 μM) modestly but significantly enhances FSK-stimulated cAMP levels ( $P < 0.001$ ). Data are representative of 10 independent experiments. (C) CP55940 (10 nM) inhibits FSK-stimulated cAMP accumulation, and this inhibition was occluded by co-application of NADA (32 μM).

accumulation ( $P=0.011$ ,  $n=3$ ), suggesting that these effects were occurring via a mechanism unrelated to CB<sub>1</sub> receptor activity. NADA was then tested for its ability to antagonize CP55940-mediated inhibition of cAMP. Consistent with a weak

interaction of NADA with hCB<sub>1</sub> receptors in these conditions, 32  $\mu$ M NADA blocked the inhibition of FSK-stimulated cAMP activity by CP55940 (10 nM) ( $P=0.003$ ,  $n=4$ ) (Figure 2C), while 10  $\mu$ M NADA was without effect ( $P=0.15$ ). It is, however, difficult to know how much of the effect of 32  $\mu$ M NADA was due to reversal of CB<sub>1</sub> receptor-mediated inhibition of FSK-stimulated AC activity by CP55940 or due to the modest CB<sub>1</sub> receptor-independent stimulation of AC activity by NADA. Finally, we examined if NADA could inhibit SR141716A-mediated inverse agonism. SR141716A (40 nM) produced an increase in cAMP in the presence of FSK which was not affected by inclusion of NADA (1–32  $\mu$ M,  $P=0.627$ – $0.985$ ,  $n=5$ ).

Another ubiquitous signalling pathway for CB<sub>1</sub> receptors is stimulation of ERK1/2 phosphorylation. While generally CB<sub>1</sub> agonists produce a pertussis toxin-sensitive pERK1/2 response, CB<sub>1</sub> receptor-mediated G-protein independent responses have also been measured (Ahn *et al.*, 2013); therefore, we examined if NADA could activate either of these pathways. As expected, in HEK 293-hCB<sub>1</sub> cells, CP55940 produced a robust stimulation of pERK, with an EC<sub>50</sub> at 5 min of  $1.7 \pm 0.7$  nM ( $n=4$ ), administration of CP55940 at approximate EC<sub>90</sub> (15 nM) produced a significant increase in ERK1/2 phosphorylation between 2 and 10 min after application, with a peak increase at 4–5 min (Figure 3,  $n=4$ ). NADA (30  $\mu$ M) did not stimulate ERK 1/2 phosphorylation at any time (Figure 3, repeated measures ANOVA showed that at 4 min, there was a significant difference in pERK phosphorylation between CP55940 and vehicle ( $P=0.033$ ) and CP55940 and NADA ( $P=0.021$ ), but not between NADA and vehicle  $P=0.503$ ).

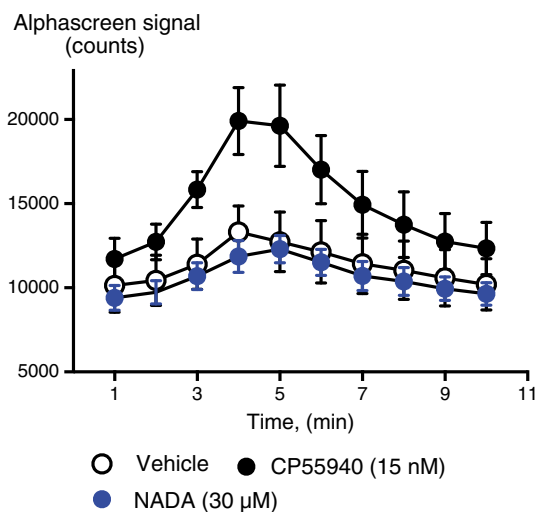


**Figure 3**

NADA does not modulate ERK phosphorylation via CB<sub>1</sub> receptors in HEK 293-hCB<sub>1</sub> cells. ERK1/2 phosphorylation was determined as outlined in the Methods. The time plot represents the fluorescent signal arising from phosphorylated ERK1/2 measured every minute after drug addition ( $T=0$ ). CP55940 ( $P=0.033$ ) but not NADA ( $P=0.503$ ) produced a significant increase in ERK1/2 phosphorylation compared with vehicle at 5 min. The data presented are the mean  $\pm$  SEM of four experiments, each performed in duplicate.

These data from multiple cell types suggested a weak interaction of NADA with human CB<sub>1</sub> receptors, so we confirmed that NADA did indeed bind to hCB<sub>1</sub> receptors using radioligand binding assays. NADA displaced both [<sup>3</sup>H]-CP55940 ( $K_i$   $780 \pm 240$  nM) and [<sup>3</sup>H]-SR141716A ( $K_i$   $230 \pm 36$  nM) from hCB<sub>1</sub> receptors ( $n=4$ ), with an affinity similar to that previously reported for rat brain receptors (Bisogno *et al.*, 2000).

Our data suggest that NADA does not readily activate G<sub>i/o</sub> or G<sub>s</sub>-coupled signalling pathways via CB<sub>1</sub> receptors. However, some cannabinoids can couple to mobilization of [Ca]<sub>i</sub> via G<sub>q</sub> (Lauckner *et al.*, 2005), so more in hope than expectation we examined this. We were able to detect small elevations of [Ca]<sub>i</sub> by NADA in HEK 293-rCB<sub>1</sub> cells (not shown), but the modest nature of the effect led us to examine a range of other cell lines. In CHO-hCB<sub>1</sub> cells, NADA elevated [Ca]<sub>i</sub> in a concentration-dependent manner, with a maximum increase in fluorescence of  $138 \pm 21\%$  at the highest concentration of NADA tested (100  $\mu$ M, Figure 4,  $n=8$ ). The elevation of [Ca]<sub>i</sub> by NADA (100  $\mu$ M) was completely prevented by pre-incubation with SR141716A (1  $\mu$ M, Figure 4,  $n=5$ ). High concentrations of the prototypic synthetic cannabinoid agonists CP55940 (300 nM,  $37 \pm 12\%$ ) and WIN55212 (10  $\mu$ M,  $40 \pm 8\%$ ) also produced elevations of [Ca]<sub>i</sub> in CHO-hCB<sub>1</sub> cells, but to a much lesser extent. As this is a considerably less potent effect than reported in N18TG2 cells, we attempted to reproduce the original report of NADA-mediated elevations of [Ca]<sub>i</sub> in these cells (Bisogno *et al.*, 2000). NADA (30  $\mu$ M) produced a maximum change in fluorescence of  $6 \pm 5\%$  in N18TG2 cells when experiments were performed at 37°C (Figure 4,  $n=6$ ). By contrast, ATP (100  $\mu$ M) and bradykinin (1  $\mu$ M) produced increases of  $51 \pm 32\%$  and  $44 \pm 36\%$  respectively (Figure 4,  $n=5$ – $6$ ). When experiments were performed at 25°C, a temperature similar to that of the original report, the increases in fluorescence produced by NADA, ATP and BK were  $5 \pm 6\%$ ,  $56 \pm 19\%$  and  $30 \pm 9\%$  respectively ( $n=3$ – $5$ ). NADA robustly elevated [Ca]<sub>i</sub> in HEK 293-hTRPV1 cells, indicating that NADA was active under the experimental conditions used to probe activity at CB<sub>1</sub> receptors (Supporting Information Fig. S1).

The increase in [Ca]<sub>i</sub> elicited by NADA in CHO-hCB<sub>1</sub> cells was independent of G<sub>i/o</sub> as it was unaffected in pertussis toxin-treated hCB<sub>1</sub> cells (Figure 5A and B). Pretreating the CHO-hCB<sub>1</sub> cells with the PLC-pathway inhibitor U73122 (3  $\mu$ M) strongly inhibited the elevation of [Ca]<sub>i</sub> by NADA 100  $\mu$ M ( $P < 0.05$ , Figure 5A and B). Pre-incubation of the CHO-hCB<sub>1</sub> cells with thapsigargin (10  $\mu$ M), a sarcoplasmic reticulum Ca pump inhibitor which depletes intracellular Ca pools, completely occluded any elevation of [Ca]<sub>i</sub> by NADA (100  $\mu$ M), confirming that NADA is mobilizing Ca from intracellular pools.

There are few readily available compounds to pharmacologically disrupt the coupling of GPCRs to G<sub>q</sub>. We used a palmitoylated peptide (palmitoyl-QLNLKEYNIV) (Robbins *et al.*, 2006), corresponding to the last 10 amino acids of G<sub>q</sub>, to test the involvement of G<sub>q</sub> in the NADA-evoked elevation of [Ca]<sub>i</sub>. Pre-incubation of the G<sub>q</sub> palpeptide (10  $\mu$ M) for an hour before the administration of NADA (30  $\mu$ M) resulted in significant inhibition of the NADA elevation of [Ca]<sub>i</sub> ( $P=0.006$ ), (Figure 5C and D). Pre-incubation with a scrambled version of the palpeptide (palmitoyl-NLVLNEKIYQ) did not significantly affect the increase in [Ca]<sub>i</sub> produced by NADA (30  $\mu$ M, Figure 5C and D,  $P=0.18$ ).

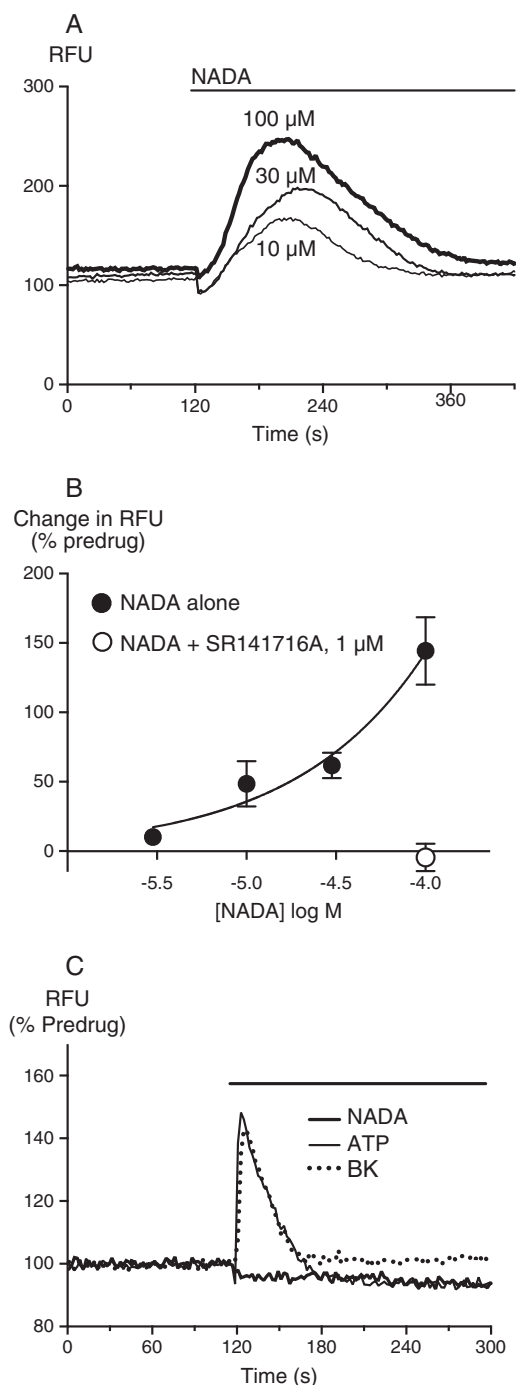


**Figure 4**

NADA elevates  $[\text{Ca}]_i$  in CHO-hCB<sub>1</sub> but not N18TG2 cells. Changes in  $[\text{Ca}]_i$  were determined as outlined in the Methods. (A) Raw traces showing increases in the fluorescent signal from the calcium 5 dye (raw fluorescence units, RFU) in CHO-hCB<sub>1</sub> cells during application of NADA. Drug was added for the duration of the bar, and the traces are representative of at least five independent experiments. (B) Concentration-response relationship for NADA elevation of  $[\text{Ca}]_i$  in CHO-hCB<sub>1</sub> cells. Data represent the mean  $\pm$  SEM of at least five independent experiments performed in duplicate or triplicate. (C) Traces illustrating the effects of NADA, ATP and bradykinin on  $[\text{Ca}]_i$  in N18TG2 cells, drugs were added for the duration of the bar and the traces are representative of at least five independent experiments.

As the NADA effects were only readily observed in CHO cells, we carried out additional experiments to determine if NADA could signal through G<sub>i/o</sub>-type G proteins in CHO-hCB<sub>1</sub>. We examined the CB<sub>1</sub> receptor-mediated inhibition of FSK-stimulated AC activity in intact CHO cells using an assay of membrane potential. We have previously reported that CHO cells hyperpolarize in response to AC activation, and this hyperpolarization can be reversed by activation of the G<sub>i</sub>/G<sub>o</sub>-coupled  $\mu$ -opioid receptor (Knapman *et al.*, 2014). FSK-hyperpolarized CHO-hCB<sub>1</sub> cells with a  $p\text{EC}_{50}$  of  $6.7 \pm 0.1$ , and a maximum change in fluorescence of  $23 \pm 2\%$  (Figure 6A,  $n = 4$ ). CP55940 (30 nM) completely inhibited the hyperpolarization produced by FSK (1  $\mu\text{M}$ ); cells hyperpolarized by  $20 \pm 1\%$  in response to FSK, and by  $-3 \pm 2\%$  in response to FSK and CP55940 together ( $n = 11$ , Figure 6B). By contrast, NADA (30  $\mu\text{M}$ ) did not affect the FSK-induced hyperpolarization in CHO-hCB<sub>1</sub> cells (Figure 6C,  $P = 0.4$ ,  $n = 6$ ). The effects of CP55940 were abolished after treatment of the cells overnight with pertussis toxin (200 ng·mL<sup>-1</sup>, Figure 6D).

Receptor internalization is a signalling pathway which is generally activated by agonists, regardless of which signalling pathway they are activating; therefore, we examined whether NADA modified cell surface hCB<sub>1</sub> receptor levels. At concentrations up to 32  $\mu\text{M}$ , NADA failed to change the levels of cell surface hCB<sub>1</sub> receptors in HEK 293 cells over 60 min ( $P = 0.137\text{--}0.936$ ,  $n = 3$ , Figure 7A). Although 100  $\mu\text{M}$  NADA induced significant CB<sub>1</sub> receptor internalization ( $29 \pm 2\%$ ,  $P < 0.006$ ,  $n = 3$ ), this was not blocked by CB<sub>1</sub> antagonist (SR141716A 100 nM,  $P = 0.602$ ,  $n = 3$ ) indicating that this was unlikely to represent a CB<sub>1</sub> receptor-mediated effect. As previously reported (Grimsey *et al.*, 2008), incubation with an approximate EC<sub>80</sub> concentration of CP55940 (1 nM) stimulated internalization of CB<sub>1</sub> receptors, with only  $17 \pm 7\%$  receptors remaining on the cell surface after 60 min. Co-application of NADA with CP55940 antagonized CP55940-induced internalization of CB<sub>1</sub> receptors, with a notional  $p\text{IC}_{50}$  of  $4.4 \pm 0.2$  ( $n = 3$ ; sigmoidal curves fitted with upper plateau constrained to 100%, Figure 7A), consistent with the ability of NADA to displace CP55940 at CB<sub>1</sub> receptors. When applied for 6 h, NADA down-regulated surface hCB<sub>1</sub> receptors in HEK 293 cells with  $p\text{EC}_{50}$   $4.49 \pm 0.01$  and maximum reduction in surface expression of  $76 \pm 5\%$  at 100  $\mu\text{M}$  NADA (Figure 7B). To investigate whether this reduction in surface expression was specific to CB<sub>1</sub> receptors, we assessed the effect of NADA on HEK 293 cells expressing the h $\beta_2$  adrenoceptor, which is not expected to bind NADA. NADA at 32  $\mu\text{M}$  produced a change in h $\beta_2$  adrenoceptor expression ( $P = 0.03$ ,  $n = 3$ ); however, the extent of the down-regulation was small in comparison with the effect on CB<sub>1</sub> receptors at the same concentration ( $\beta_2$  adrenoceptor  $13 \pm 3\%$ , CB<sub>1</sub> receptor  $54 \pm 5\%$ ,  $n = 3$ ). A substantial reduction was observed at 100  $\mu\text{M}$  NADA ( $48 \pm 3\%$ ;  $P = 0.018$ ,  $n = 3$ , Figure 7B). We also noted a small but significant reduction in cell count ( $14 \pm 3\%$ ,  $P = 0.006$ ,  $n = 3$ ) indicating that cell viability may have been adversely affected at this high concentration; 100  $\mu\text{M}$  NADA produced a similar effect on cell number in untransfected HEK 293 cells ( $11 \pm 2\%$  reduction in cell number). These data suggest that 100  $\mu\text{M}$  NADA has non-specific effects on cell viability and receptor trafficking. However, as it appeared that 32  $\mu\text{M}$  NADA induced a specific reduction of cell surface CB<sub>1</sub> receptors, evident following 6 h but not 1 h of stimulation, considerably slower than would be typical for agonist stimulation (Grimsey *et al.*, 2008), we were curious to determine the rate at which this occurred. Time course experiments (Figure 7C)

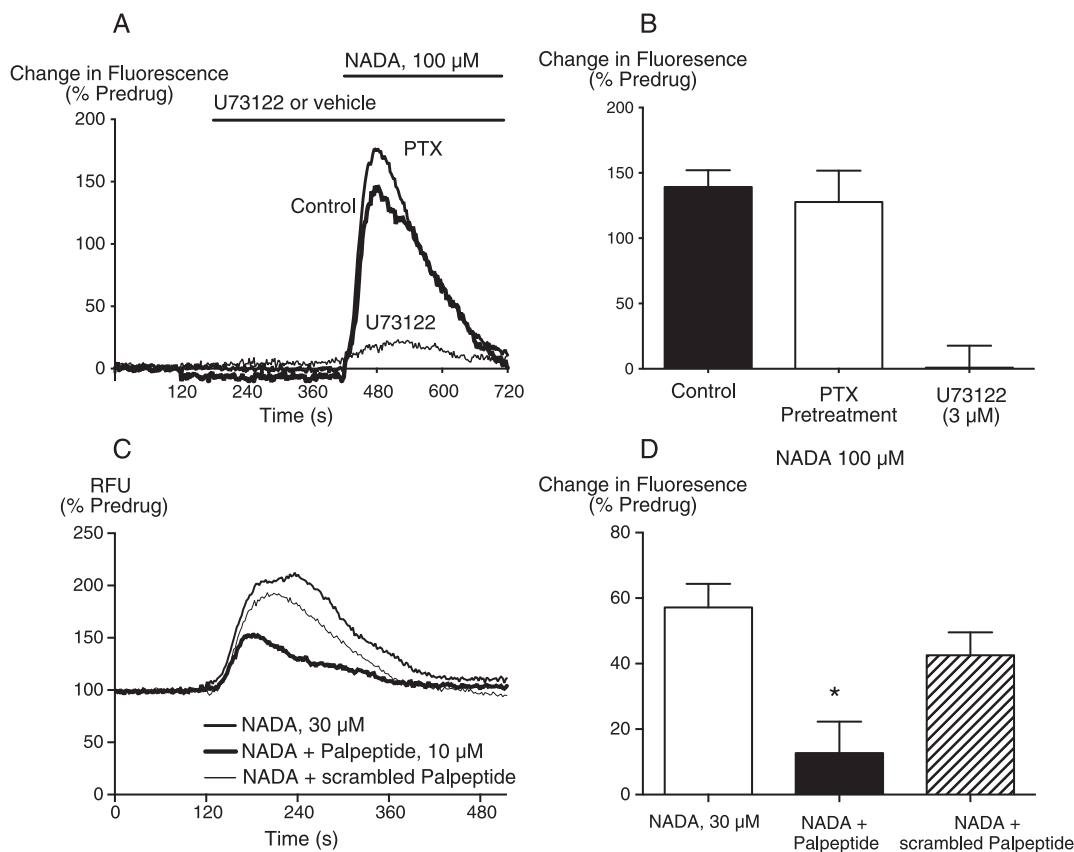


## Figure 5

NADA elevates  $[Ca]_i$  in a manner consistent with activation of  $G_q$ . Changes in  $[Ca]_i$  were measured as described in the Methods. (A) Traces from a representative experiment showing that elevations of  $[Ca]_i$  were inhibited by U73122, but not affected by pretreatment with pertussis toxin overnight. (B) Summary of the data from five similar experiments, expressed as mean  $\pm$  SEM. (C) Traces from a representative experiment showing that elevations of  $[Ca]_i$  were attenuated by a peptide antagonist of  $G_q$  (palpeptide) but not by the scrambled palpeptide control. (D) Summary of the data from five similar experiments, the  $G_q$  palpeptide significantly inhibited the elevations of  $[Ca]_i$  in response to 30  $\mu$ M NADA, ( $P = 0.006$ ).

revealed that the initiation of down-regulation of surface  $CB_1$  receptors appeared to be considerably delayed, and the subsequent rate of  $CB_1$  receptor loss was also slower in comparison with that stimulated by 10 nM CP55940. Qualitatively, similar results were found in CHO-h $CB_1$  cells indicating that the stimulation of  $G_q$  in these cells did not alter the internalization of the receptor (data not shown).

## Discussion

The principal finding of this study is that NADA, a putative endogenous agonist for  $CB_1$  receptors, couples effectively to a limited range of effectors in cells expressing recombinant human or rat  $CB_1$  receptors. We were unable to detect any coupling to  $G_i/G_o$ - or  $G_s$ -mediated processes, but we did observe elevations of  $[Ca]_i$  consistent with  $G_q$ -mediated stimulation of phospholipase C and subsequent mobilization of thapsigargin-sensitive intracellular Ca stores. Recombinant r $CB_1$  receptors can couple through  $G_q$  in HEK 293 cells (Lauckner *et al.*, 2005), and while WIN55212 has been reported to be the most

effective agonist at this pathway, no  $CB$  ligands with appreciable  $G_q$ -selectivity have previously been identified. The only previous  $CB_1$  receptor-mediated signalling pathway identified for NADA was an elevation of  $[Ca]_i$  following activation of native mouse  $CB_1$  receptors in N18TG2 cells (Bisogno *et al.*, 2000). Although the G protein mediating this effect was not identified in that study, others using related NG108-15 neuroblastoma cells indicate that this elevation of  $[Ca]_i$  is probably mediated by PTX-sensitive G proteins (Sugiura *et al.*, 1997). We were unable to reproduce the NADA-mediated elevations of  $[Ca]_i$  reported by Bisogno *et al.* (2000); this probably reflects the quite different assay conditions. In the original study, the N18TG2 cells were acutely treated with trypsin and resuspended in a continuously stirred cuvette where drugs were added and measurements of  $[Ca]_i$  made. By contrast, the cells in our study were attached to a tissue culture plate and drugs added very gently after at least an hour of equilibration between dye and cells within the Flexstation. Although we do not know which differences are crucial, we note that it has been previously reported that  $CB_1$  receptors can couple to elevations of  $[Ca]_i$  when added under conditions where a  $G_q$ -coupled receptor is activated (Marini *et al.*, 2009). Stirring cells in a cuvette has also been



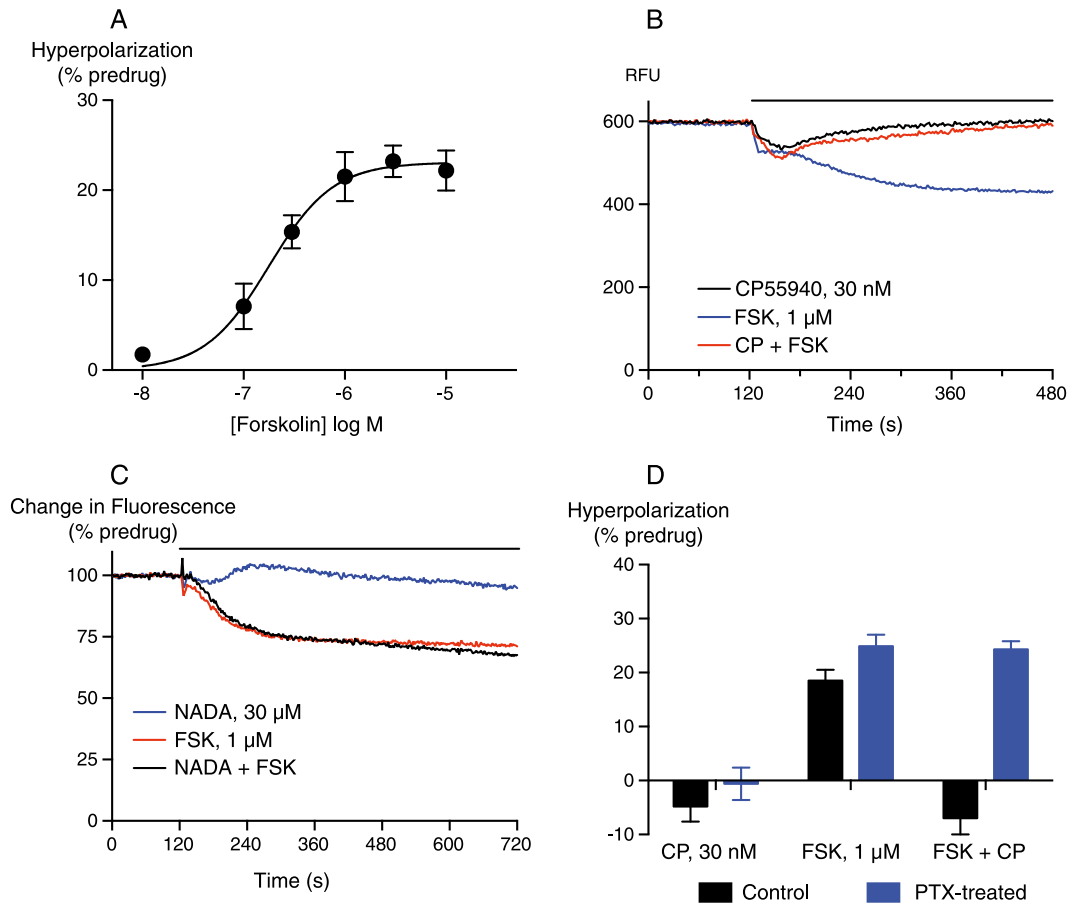


## Figure 6

NADA does not modulate adenylyl cyclase activity in CHO-hCB<sub>1</sub> cells. Adenylyl cyclase activity was determined using a membrane potential assay, as outlined in the Methods. (A) A concentration-response relationship for FSK hyperpolarization of CHO-hCB<sub>1</sub> cells. FSK-hyperpolarized cells with a  $pEC_{50}$  of 6.7. Data were fit with a four-parameter logistic equation, and each point represents the mean  $\pm$  SEM of four independent experiments performed in duplicate. (B) A representative experiment showing raw fluorescence traces (RFU) of FSK-induced hyperpolarization of CHO-hCB<sub>1</sub> cells, and its reversal by CP55940. Drugs were added for the duration of the bar. (C) Normalized traces from a representative experiment (of 12) showing the lack of effect of NADA (30  $\mu$ M) on the FSK-induced hyperpolarization. The solvent blank trace has been subtracted from this data. (D) A bar chart summarizing the inhibitory activity of CP55940 (30 nM) on FSK-stimulated hyperpolarization of CHO-hCB<sub>1</sub> cells, in control conditions and after overnight treatment of cells with 200 ng·mL<sup>-1</sup> pertussis toxin (PTX). The bars represent the mean  $\pm$  SEM of five or six independent experiments, each performed in duplicate or quadruplicate.

reported to produce a release of substances such as ATP which act in this manner to permit G<sub>i</sub>/G<sub>o</sub>-coupled receptor elevations of [Ca]<sub>i</sub> (Okajima *et al.*, 1993). It is thus possible that NADA was acting as a CB<sub>1</sub> agonist in a situation where there was an ongoing G<sub>q</sub>-coupled receptor activity permissive for pertussis toxin-sensitive elevations of [Ca]<sub>i</sub>.

The effects of NADA on [Ca]<sub>i</sub> were not very potent, with robust elevations only occurring at concentrations of 30  $\mu$ M and above. In N18TG2 cells, NADA mobilized Ca via CB<sub>1</sub> receptors with an EC<sub>50</sub> of about 700 nM (Bisogno *et al.*, 2000), while in brain slices significant effects of NADA on synaptic transmission have been reported at concentrations between 1 and 10  $\mu$ M (Marinelli *et al.*, 2007, Fawley *et al.*, 2014). The affinity of NADA for native rCB<sub>1</sub> was reported to be 250 nM (vs. [<sup>3</sup>H]-SR141716A, Bisogno *et al.*, 2000); in the present study, the K<sub>i</sub> for NADA was 230 nM versus [<sup>3</sup>H]-SR141716A, and 780 nM for the agonist

[<sup>3</sup>H]-CP55940. Thus, the mobilization of [Ca]<sub>i</sub> we observed occurred at much higher concentrations than effects in brain slices and in radioligand binding assays, notwithstanding the potential differences arising from the different assays. Given that 30  $\mu$ M NADA had no effect at all on other signalling pathways we measured, our data suggest either that NADA couples more efficiently to G<sub>q</sub> in nerve terminals than in whole CHO cells (or that the consequences of small changes in [Ca]<sub>i</sub> in nerve terminals are magnified as effects on neurotransmitter release), or that the NADA modulation of neurotransmitter release in brain slices does not involve modulation of AC, ERK or GIRK activity and proceeds through other mechanisms.

We have provided evidence consistent with NADA utilizing G<sub>q</sub>-family G proteins to mediate elevation of [Ca]<sub>i</sub>, but we do not have direct evidence. The elevation of [Ca]<sub>i</sub> was not mediated via pertussis toxin-sensitive G proteins, ruling out

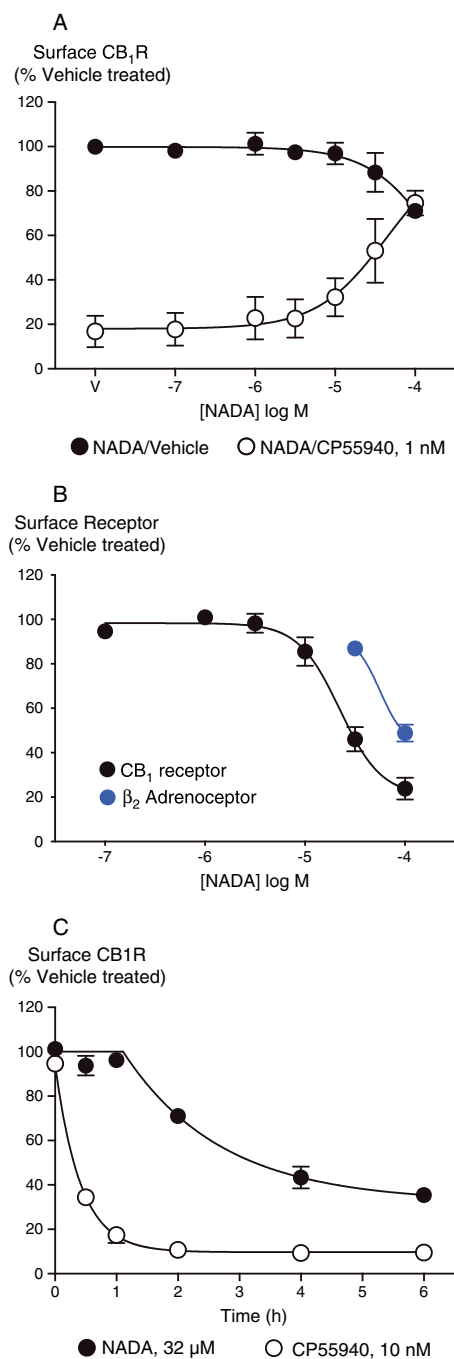


**Figure 7**

NADA modulates CB<sub>1</sub> receptor surface expression in HEK 293-hCB<sub>1</sub> cells. CB<sub>1</sub> surface expression was determined as outlined in the Methods. Data represent the mean ± SEM of three independent experiments performed in duplicate and normalized to vehicle control (V). (A) When incubated for 1 h, NADA alone induced significant internalization only at the highest concentration tested (100 μM,  $P < 0.006$ ). 1 nM CP55940 induced internalization which was inhibited by co-incubation of NADA ( $p_{IC50} 4.4 \pm 0.2$ ). (B) Incubation for 6 h with NADA induced a down-regulation of surface CB<sub>1</sub> receptors ( $p_{EC50} 4.49 \pm 0.01$ ), and also loss of cell surface β<sub>2</sub>-adrenoceptors. (C) Timecourse of 32 μM NADA and 10 nM CP55940 effects on the expression of surface CB<sub>1</sub> receptors.

mechanisms observed in NG108-15 cells. The NADA-mediated elevations of [Ca]<sub>i</sub> were disrupted by U73122, an antagonist of G<sub>q</sub>-PLC signalling in a number of systems, including CB<sub>1</sub> receptor-mediated G<sub>q</sub> coupling (Lauckner *et al.*, 2005). The elevations of [Ca]<sub>i</sub> produced by NADA were also occluded by thapsigargin, an agent which depletes intracellular Ca stores. Finally, the elevations of [Ca]<sub>i</sub> were largely occluded by a G<sub>q</sub> palpeptide, a palmitoylated peptide corresponding to the last 10 amino acids of G<sub>q</sub> that is purported to act as a competitive inhibitor of G<sub>q</sub>-PLC interactions (Robbins *et al.*, 2006). Taken together, these data strongly suggest an involvement of G<sub>q</sub> in NADA signalling via CB<sub>1</sub> receptors, at least in CHO cells.

Mobilization of Ca by native CB<sub>1</sub> receptors has been observed occasionally (Sugiura *et al.*, 1997; Bisogno *et al.*, 2000; McIntosh *et al.*, 2007; Marini *et al.*, 2009), but the physiological consequences of this remain largely unknown. Ca is a second messenger that can modulate many cellular processes through activation of protein kinases, phosphatases and transcription factors, while changes in [Ca]<sub>i</sub> can also activate or inhibit ion channels to alter cellular excitability. The mechanism(s) of action of NADA modulation of neurotransmitter release in native neurons are unknown, beyond demonstration of the involvement of CB<sub>1</sub> receptors and/or TRPV1 (Price *et al.*, 2004; Marinelli *et al.*, 2007; Fawley *et al.*, 2014; Freestone *et al.*, 2014). Given that NADA does not seem to readily couple to conventional second messengers such as AC, ERK or K channels, it is an intriguing possibility that the effects of NADA can in some cases be mediated by NADA/CB<sub>1</sub>/G<sub>q</sub> coupling, perhaps by 2-AG or AEA generated as a result of the elevations of [Ca]<sub>i</sub> or liberation of fatty acids. Evidence to support the idea of NADA-mediated elevations of [Ca]<sub>i</sub> being relevant in actions on neurons comes from the observation that NADA-stimulated CGRP release from trigeminal ganglion neurons in conditions where NADA-mediated TRPV1 activation is completely blocked (Price *et al.*, 2004). However, putative NADA-dependent cannabinoid tone in the substantia nigra was not sensitive to inhibition of 2-arachidonoyl glycerol synthesis (Freestone *et al.*, 2014), indicating that NADA did not elevate 2-AG levels via a G<sub>q</sub>-dependent process in this brain region. In preliminary experiments in CHO-hCB<sub>1</sub> cells, we found that brief NADA exposure (up to 10 min) did indeed cause a modest elevation in levels of 2-AG; however, the effects of NADA were not sensitive to SR141716A and persisted in wild-type CHO cells (data not shown). These actions could reflect NADA inhibition of monoacylglycerol lipase, a principle catabolic enzyme for 2-AG (Bjorkland *et al.*, 2010).

NADA acts via cannabinoid receptor-dependent mechanisms in non-neuronal cells (O'Sullivan *et al.*, 2004; Wilhelmsen *et al.*, 2014), but there is also no information as to the signalling pathways used by NADA in these situations. A plethora of non-CB receptor, non-TRPV1-mediated effects of NADA have been reported, including direct actions on ion channels, lipid-modifying enzymes, transcription factors and possibly other GPCR (e.g. Ross *et al.*, 2009; Bjorkland *et al.*, 2010; Soler-Torronteras *et al.*, 2014; reviewed in Connor *et al.*, 2010). None of these effects are likely to lead to rapid elevations of [Ca]<sub>i</sub>, nor are they likely to acutely interfere with conventional CB<sub>1</sub> receptor signalling pathways.

Evidence is emerging for ligand bias at CB<sub>1</sub> receptors, particularly with respect to arrestin recruitment and activation of pathways downstream of this such as ERK (Laprairie *et al.*, 2014; Khajehali *et al.*, 2015). The only coupling we could

observe with NADA appeared to be via  $G_q$ , suggesting that NADA is a highly biased agonist. Although WIN55212 has been reported to be the most efficient cannabinoid at promoting elevations of  $[Ca]_i$  via  $G_q$  (Lauckner *et al.*, 2005; McIntosh *et al.*, 2007), unlike NADA, WIN55212 also couples effectively to  $G_i/G_o$  and  $G_s$  (Bonhaus *et al.*, 1998; Glass and Northrup, 1999; Laprairie *et al.*, 2014). In some cell types, all  $CB_1$  agonists can promote  $G_q$ -dependent signalling (Laprairie *et al.*, 2014), although this is not always observed (McIntosh *et al.*, 2007). However, it is not possible to quantify bias for NADA, as we were unable to detect coupling to other pathways. The lack of any other *in vitro* reports of NADA coupling to  $CB_1$  receptors suggests measuring them may not be straightforward, and we await confirmation of our results with interest. It remains possible that NADA can couple to more commonly observed  $CB_1$  receptor signal transduction cascades, perhaps in the presence of as yet unidentified regulators of  $CB_1$  receptor coupling.

It is important to note that positive controls were used in all experiments, and the robust activity of the cannabinoid agonists CP55940 or WIN55212 indicated that the  $CB_1$  receptors were functional during these experiments, notwithstanding the many papers we (and others) have published using these receptor constructs and signalling assays. Furthermore, we measured NADA activation of hTRPV1 under the same conditions as our assays of  $[Ca]_i$  in CHO-h $CB_1$ , HEK 293-h $CB_1$  and N18TG2 cells, and NADA activated the channel in a manner consistent with previous reports (Huang *et al.*, 2002; Sutton *et al.*, 2005), indicating that it was not metabolized too rapidly to act. The assays we used are well characterized and can reliably detect the activity of lower efficacy  $CB_1$  agonists such as  $\Delta^9$  tetrahydrocannabinol and anandamide (Banister *et al.*, 2013; Cawston *et al.*, 2013).

Despite the apparent lack of coupling to canonical  $CB_1$  receptor signalling pathways and low potency for elevating elevation of  $[Ca]_i$ , the ability of NADA to displace orthosteric  $CB_1$  ligands (Bisogno *et al.*, 2000, this study) indicates that NADA may be able to influence the activity of other cannabinoids by acting as a competitive antagonist. Indeed, NADA inhibited internalization of  $CB_1$  receptors induced by CP55940. Although this effect also occurred with fairly low potency, it illustrates the potential for NADA to subtly influence endocannabinoid tone by antagonizing canonical signalling pathways while simultaneously inducing Ca signalling. Interestingly, although NADA did not stimulate rapid internalization of  $CB_1$  receptors as usually expected of  $CB_1$  agonists (Grimsey *et al.*, 2008), the delayed down-regulation of surface  $CB_1$  receptors was induced with a similar potency to the inhibition of CP55940-stimulated internalization. Thus, as well as the potential for competitive inhibition, the prolonged presence of NADA down-regulates surface  $CB_1$  receptors and is likely to functionally desensitize surface  $CB_1$  receptor-mediated signalling. The apparent lag to the start of down-regulation and subsequent slow decay is reminiscent of what is observed with application of low concentrations of efficacious agonists (Grimsey *et al.*, 2008). NADA may inefficiently stabilize a  $CB_1$  receptor conformation that is recognized by internalization machinery, resulting in a slow internalization rate. Alternatively, NADA may influence other aspects of cell function or endocannabinoid tone, as discussed previously. A very high NADA concentration (100  $\mu$ M) produced non- $CB_1$  receptor-mediated reductions in surface expression of the  $\beta_2$  adrenoceptor and cell density, both of which probably reflect reduced cell viability.

In summary, NADA appears to represent a  $CB_1$  ligand that preferentially accesses conformations of the receptor which activate  $G_q$ , suggesting that it might be possible to develop analogous drugs. NADA may also represent a useful tool for investigating the consequences of  $CB_1$  receptor- $G_q$  coupling in native systems. Our data do not directly address the importance of NADA as an endogenous cannabinoid, but the high concentrations of NADA required to stimulate detectable activation of any conventional G protein-coupled pathways suggests that if endogenous NADA acts widely as an endocannabinoid, it does so through as yet unidentified signalling mechanisms. Despite evidence for the endogenous production of NADA (Huang *et al.*, 2002; Bradshaw *et al.*, 2006; Freestone *et al.*, 2014), its role as an endocannabinoid remains unclear.

## Author contributions

All authors performed experiments and contributed to the analysis and interpretation the data. W.J.R. and M.C. largely wrote the paper; all authors have seen a final copy of the Ms.

## Conflict of interest

The authors declare that they have no conflicts of interest related to this work.

## References

- Ahn KW, Mahmoud MM, Shim J-Y, Kendall DA (2013). Distinct roles of  $\beta$ -arrestin 1 and  $\beta$ -arrestin 2 in ORG27569-induced biased signalling and internalization of the cannabinoid receptor 1 ( $CB_1$ ). *J Biol Chem* 288: 9790–9800.
- Alexander SP, Benson HE, Faccenda E, Pawson AJ, Sharman JL, Spedding M *et al.* (2013a). The Concise Guide to PHARMACOLOGY 2013/14: G protein-coupled receptors. *Br J Pharmacol* 170: 1449–58.
- Alexander SP, Benson HE, Faccenda E, Pawson AJ, Sharman JL, Catterall WA *et al.* (2013b). The concise guide to pharmacology 2013/14: ion channels. *Br J Pharmacol* 170: 1607–1651.
- Alexander SP, Benson HE, Faccenda E, Pawson AJ, Sharman JL, Spedding M *et al.* (2013c). The concise guide to PHARMACOLOGY 2013/14: enzymes. *Br J Pharmacol* 170: 1797–1867.
- Alexander SP, Kendall DA (2007). The complications of promiscuity: endocannabinoid action and metabolism. *Br J Pharmacol* 152: 602–623.
- Banister S, Wilkinson S, Longworth M, Stuart J, Apetz N, English K *et al.* (2013). The synthesis and pharmacological evaluation of adamantane-derived indoles: novel cannabimimetic drugs of abuse. *ACS Chem Neurosci* 4: 1081–1092.
- Bisogno T, Melck D, Bobrov MY, Gretskey NM, Bezuglov VV, De Petrocellis L *et al.* (2000). *N*-acyl-dopamines: novel synthetic  $CB_1$  cannabinoid-receptor ligands and inhibitors of anandamide inactivation with cannabimimetic activity *in vitro* and *in vivo*. *Biochem J* 351: 817–814.
- Bjorkland E, Noren E, Nilsson J, Fowler CJ (2010). Inhibition of monoacylglycerol lipase by troglitazone, *N*-arachidonoyl dopamine

- and the irreversible inhibitor JZL184: comparison of two different assays. *Br J Pharmacol* 161: 1512–1526.
- Bonhaus DW, Chang LK, Kwan J, Martin GR (1998). Dual activation and inhibition of adenylyl cyclase by cannabinoid receptor agonists: evidence for agonist-specific trafficking of intracellular responses. *J Pharmacol Exp Ther* 287: 884–888.
- Bradshaw HB, Rimmerman N, Krey JE, Walker JM (2006). Sex and hormonal cycle differences in rat brain levels of pain-related cannabimimetic lipid mediators. *Am J Physiol Regul Integr Comp Physiol* 291: R349–R358.
- Cawston EE, Redmond WJ, Breen C, Grimsey N, Connor M, Glass M (2013). Real-time characterisation of cannabinoid receptor 1 (CB1) allosteric modulators reveals novel mechanism of action. *Br J Pharmacol* 170: 893–907.
- Connor M, Vaughan CW, Vandenberg R (2010). *N*-Acyl amino acids and *N*-acyl neurotransmitter conjugates: neuromodulators and probes for new drug targets. *Br J Pharmacol* 160: 1857–1871.
- Fawley JA, Hofmann ME, Andresen MC (2014). Cannabinoid 1 and transient receptor potential vanilloid 1 receptors discretely modulate evoked glutamate separately from spontaneous glutamate transmission. *J Neurosci* 34: 8324–8332.
- Felder CC, Briley EM, Axelrod J, Simpson JT, Mackie K, Devane WA (1993). Anandamide, an endogenous cannabimimetic eicosanoid, binds to the cloned human cannabinoid receptor and stimulates receptor-mediated signal transduction. *Proc Natl Acad Sci U S A* 90: 7656–7660.
- Freestone PS, Guatteo E, Piscitelli F, di Marzo V, Lipski J, Mercuri N (2014). Glutamate spillover drives endocannabinoids production and inhibits GABAergic transmission in the Substantia Nigra pars compacta. *Neuropharmacology* 79: 467–475.
- Glass M, Felder CC (1997). Concurrent stimulation of cannabinoid CB1 and dopamine D2 receptors augments cAMP accumulation in striatal neurons: evidence for a Gs linkage to the CB1 receptor. *J Neurosci* 17: 5327–5333.
- Glass M, Northrup JK (1999). Agonist selective regulation of G proteins by cannabinoid CB<sub>1</sub> and CB<sub>2</sub> receptors. *Mol Pharmacol* 56: 1362–1369.
- Grimsey NL, Narayan PJ, Dragunow M, Glass M (2008). A novel high-throughput assay for the quantitative assessment of receptor trafficking. *Clin Exp Pharm Physiol* 35: 1377–1382.
- Grimsey NL, Graham ES, Dragunow M, Glass M (2010). Cannabinoid receptor 1 trafficking and the role of the intracellular pool: implications for therapeutics. *Biochem Pharmacol* 80: 1050–1062.
- Hohmann AG, Suplita RL, Bolton NM, Neely MH, Fegley D, Mangieri R *et al.* (2005). An endocannabinoid mechanism for stress-induced analgesia. *Nature* 435: 1108–1112.
- Hu SS, Bradshaw HB, Benton VM, Chen JS, Huang SM, Minassi A *et al.* (2009). The biosynthesis of *N*-arachidonoyl dopamine (NADA), a putative endocannabinoid and endovanilloid, via conjugation of arachidonic acid with dopamine. *Prostaglandins Leukot Essential Fatty Acids* 81: 291–301.
- Huang SM, Bisogno T, Trevisani M, Al-Hayani A, de Petrocellis L, Fezza F *et al.* (2002). An endogenous capsaicin-like substance with high potency at recombinant and native vanilloid receptors. *Proc Natl Acad Sci U S A* 99: 8400–8405.
- Hudson BD, Hebert TE, Kelly MEM (2010). Ligand-and heterodimer-directed signalling of the CB1 cannabinoid receptor. *Mol Pharmacol* 77: 1–9.
- Khajehali E, Malone DT, Glass M, Sexton PM, Christopoulos A, Leach K (2015). Biased agonism and biased allosteric modulation at the CB1 cannabinoid receptor. *Mol Pharmacol* 88: 368–379.
- Knapman A, Santiago M, Du YP, Bennallack PR, Christie MJ, Connor M (2013). A continuous, fluorescence-based assay of mu-opioid receptor activation in AtT20 cells. *J Biomol Screen* 18: 269–276.
- Knapman A, Abogadie F, McIntyre P, Connor M (2014). A real time, fluorescence-based assay for measuring  $\mu$ -opioid receptor modulation of adenylyl cyclase activity in Chinese hamster ovary cells. *J Biomol Screen* 19: 223–231.
- Laprairie RB, Bagher AM, Kelly MEM, Dupre DJ, Denovan-Wright EM (2014). Type 1 cannabinoid receptor ligands display functional selectivity in cell culture model of striatal medium spiny projection neurons. *J Biol Chem* 289: 24845–24862.
- Lauckner JE, Hille B, Mackie K (2005). The cannabinoid agonist WIN55,212-2 increases intracellular calcium via CB1 receptor coupling to Gq proteins. *Proc Natl Acad Sci U S A* 102: 19144–19149.
- Lovinger DM (2008). Presynaptic modulation by endocannabinoids. In: Sudhoff TC (ed). *Pharmacology of Neurotransmitter release* Starke K. *Handb Exp Pharm* 184. Springer: Berlin, pp. 435–477.
- Mackie K (2005). Distribution of cannabinoid receptors in the central and peripheral nervous system. In: Pertwee RG (ed). *Cannabinoids* *Handb Exp Pharm* 168. Springer: Berlin, pp. 299–325.
- Mackie K, Lai Y, Westenbroek R, Mitchell R (1995). Cannabinoids activate an inwardly rectifying potassium conductance and inhibit Q-type calcium currents in AtT20 cells transfected with rat brain cannabinoid receptors. *J Neurosci* 15: 6552–6561.
- Marinelli S, Di Marzo V, Florenzano F, Fezza F, Viscomi MT, van der Selt M *et al.* (2007). *N*-Arachidonoyl-dopamine tunes synaptic transmission onto dopaminergic neurons by activating both cannabinoid and vanilloid receptors. *Neuropsychopharmacology* 32: 298–308.
- Marini P, Moriello AS, Cristino L, Palmery M, De Petrocellis L, Di Marzo V (2009). Cannabinoid CB1 receptor elevation of intracellular calcium in neuroblastoma SH-SY5Y cells: interactions with muscarinic and  $\delta$ -opioid receptors. *Biochem Biophys Acta* 1793: 1289–1303.
- McIntosh BT, Hudson B, Yergorova S, Jollimore CAB, Kelly MEM (2007). Agonist-dependent cannabinoid receptor signalling in human trabecular network cells. *Br J Pharmacol* 152: 1111–1120.
- Okajima F, Tomura H, Kondo Y (1993). Enkephalin activates the phospholipase C/ $Ca^{2+}$  system through cross-talk between opioid receptors and P2-purineric or bradykinin receptors in NG108-15 cells. *Biochem J* 290: 241–247.
- O'Sullivan SE, Kendall DA, Randall MD (2004). Characterization of the vasorelaxant properties of the novel endocannabinoid *N*-arachidonoyl dopamine (NADA). *Br J Pharmacol* 141: 803–812.
- Pawson AJ, Sharman JL, Benson HE, Faccenda E, Alexander SP, Buneman OP *et al.* (2014). The IUPHAR/BPS Guide to PHARMACOLOGY: an expert-driven knowledgebase of drug targets and their ligands. *Nucl. Acids Res.* 42 (Database Issue): D1098–106.
- Price TJ, Patwardhan A, Akopian AN, Hargreaves KM, Flores CM (2004). Modulation of trigeminal sensory neuron activity by the dual cannabinoid-vanilloid agonists anandamide, *N*-arachidonoyl dopamine and arachidonoyl-2-chloretylamide. *Br J Pharmacol* 141: 1118–1130.
- Redmond WJ, Gu L, Camo M, McIntyre P, Connor M (2014). Ligand determinants of fatty acid activation of the pronociceptive ion channel TRPA1. *PeerJ* 2: e248.

Robbins J, Marsh SJ, Brown DA (2006). Probing the regulation of M (Kv7) potassium channels in intact neurons with membrane-targeted peptides. *J Neurosci* 26: 7950–7961.

Ross HR, Gilmore AJ, Connor M (2009). Inhibition of human recombinant T-type calcium channels by the endocannabinoid arachidonyl dopamine. *Br J Pharmacol* 156: 740–750.

Soler-Torronteras R, Lara-Chica M, Garcia V, Calzado MA, Munoz E (2014). Hypoximimetic activity of *N*-acyl-dopamines. *N*-arachidonoyl dopamine stabilizes HIF1 $\alpha$  protein through a SIAH2-dependent pathway. *Biochem Biophys Acta* 1843: 2730–2743.

Sugiura T, Kodak T, Kondo S, Tonegawa T, Nakane S, Kishimoto S *et al.* (1997). 2-Arachidonoylglycerol, a putative endogenous cannabinoid receptor ligand, induces rapid, transient elevation of intracellular free Ca<sup>2+</sup> in neuroblastoma x glioma hybrid NG108-15 cells. *Biochem Biophys Res Comm* 229: 58–64.

Sutton KG, Garret EM, Rutter AR, Bonnert TP, Jarolimek W, Seabrook GR (2005). Functional characterization of the S512Y mutant vanilloid human TRPV1 receptor. *Br J Pharmacol* 146: 702–711.

Veldhuis NA, Lew MJ, Abogadie FC, Poole DP, Jennings EA, Ivanusic JJ *et al.* (2012). N-glycosylation determines the ionic permeability and desensitization of the TRPV1 capsaicin receptor. *J Biol Chem* 287: 21765–21772.

Wilhelmsen K, Khakpour S, Tran A, Sheehan K, Schumacher M, Xu F *et al.* (2014). The endocannabinoid/endovanilloid *N*-arachidonoyl dopamine (NADA) and synthetic cannabinoid WIN55,212-2 abate the inflammatory activation of human endothelial cells. *J Biol Chem* 289: 13079–13100.

## Supporting information

Additional Supporting Information may be found in the on-line version of this article at the publisher's web-site:

<http://dx.doi.org/10.1111/bph.13341>

**Figure S1** NADA activates hTRPV1 expressed in HEK 293 cells. Changes in [Ca]<sub>i</sub> were determined as outlined in the Methods. A) Traces showing increases in the fluorescent signal from the calcium 5 dye in HEK 293-hTRPV1 cells during application of NADA or capsaicin. Drug was added for the duration of the bar, the traces are representative of at least 7–8 independent experiments. B) Concentration response relationship for NADA and capsaicin elevation of [Ca]<sub>i</sub> in HEK 293-hTRPV1 cells. Data represents the mean  $\pm$  SEM of 7–8 independent experiments performed in duplicate or triplicate.